

Hafnia and Alumina on Sulphur Passivated Germanium

M. Althobaiti¹, S. Mather², N. Sedghi³,
V. R. Dhanak¹, I. Z. Mitrovic³, S. Hall³, and P. R. Chalker²

*1. Department of Physics, 2. School of Engineering, 3. Dept. of Electrical Eng. & Electronics,
University of Liverpool, Liverpool, UK*

Abstract

In this work hafnia (HfO₂) and alumina (Al₂O₃) films were deposited on germanium, using either water or oxygen plasma as the oxidant, by atomic layer deposition at 250°C with and without sulphur passivation of the substrate. X-ray photoelectron spectroscopy was carried out to investigate the interface between both HfO₂ and Al₂O₃ films and germanium. The results show that for hafnia and alumina deposited with water on pre-sulphur treated germanium there is negligible GeO_x formation when compared to films grown using oxygen plasma. The results support the case for sulphur passivation of the interface.

1. Introduction

Germanium is seen as a potential new channel material in Complementary Metal Oxide Semiconductor (CMOS) technology, due to its high hole mobility compared to Si [1,2]. It is necessary to include an ultra-thin GeO_x layer between the high-k material and the Ge substrate to maintain a good quality interface. However, such a layer inhibits scaling of the gate stack so it would be desirable to find an alternative passivation technique. Furthermore, this layer causes severe problems in processing, because of its high water solubility and thermally-unstable nature, which can result in a poor quality interface and consequently, degraded channel mobility [3]. A number of alternative methods have been suggested to passivate the Ge surface, such as nitridation, rare-earth buffer oxide layer [4], and Al₂O₃ or sulphur passivation [5]. The introduction of S in the GeO_x can result in superior Ge gate stack [6]. It has been shown for Al₂O₃/Ge stacks that depending on the oxidant precursor (H₂O or O₃) of the Atomic Layer Deposition (ALD) of Al₂O₃, the gate stack can be tuned for p-MOS (Metal Oxide Semiconductor) or nMOS applications [7]. In effect, with Al₂O₃ deposition with H₂O, no GeO_x was detected at the interface and a low density of interface states (D_{it}) has been measured at the valence band edge making this gate stack suitable for pMOS application. On the contrary, Al₂O₃ with O₃ deposition has resulted in a thin Ge-suboxide and low D_{it} at the conduction band edge making this gate

stack suitable for nMOS application [7]. In this paper, HfO₂/Ge and Al₂O₃/Ge gate stacks have been deposited by ALD using O-plasma and H₂O. Both O-plasma and O₃ as the co-reagents in ALD avoid the potential incorporation of hydrogen that is possible if using H₂O vapour. The hydroxyl incorporation has been reported for H₂O-based ALD [8]. Oxygen-plasma and O₃ have more effective pumping speeds facilitating shorter purge times than H₂O. O₃ is effectively more reactive than O-plasma, which can lead to thicker interfacial oxides at the growth temperatures of 250°C used in this work, and also can lead to more carbon incorporation from the metal precursor ligands. Therefore, O-plasma and H₂O were used as oxidants during ALD and an assessment of their effect on the S passivated germanium is the main new contribution of this work.

2. Experimental

Ge (100) n- wafers of the resistivity 0.3-3 Ωcm were degreased by ultrasonic bath in acetone and then given a cyclic HF/water rinse in order to remove the native oxide layer, followed by sulphur deposition by dipping the samples in a 20% ammonium sulphide, (NH₄)₂S, solution in water for 10 minutes and then dried under an argon flow. The samples were then immediately transferred into an Oxford Instruments OpAL ALD reactor, where 65, 130 and 250 cycles were used to deposit 3, 7 and 20 nm HfO₂ layers using [(CpMe)2HfOMeMe]

precursor coupled with remote oxygen plasma or water. The 3 nm Al_2O_3 layers were deposited in the same ALD reactor using trimethylaluminium (TMA) precursor with both O-plasma and water, as above. Note that we have also fabricated HfO_2 layers on alumina S-passivated Ge using O-plasma. For this process, S-treated samples were exposed to an Al flux for a range of times to deposit ultra-thin Al layers. The samples were then oxidized at ambient temperatures in the Molecular Beam Epitaxy (MBE) load lock to produce sub-nm (~ 0.3 nm) Al_2O_3 layers. Then, the samples were transferred to the ALD reactor, where 7 nm HfO_2 films were deposited using 130 ALD cycles using the same HfO_2 precursor and O-plasma as oxidant. As reference samples to the latter batch, 7 nm HfO_2 on S-passivated Ge were fabricated using O-plasma. The thickness of deposited HfO_2 and Al_2O_3 films was obtained using in-situ single wavelength spectroscopic ellipsometer. The Transmission Electron Microscopy (TEM) measurements were performed on 20 nm HfO_2/Ge sample prepared by focussed ion beam milling. The final thinning of the sample was carried out at 100 pA using gallium ions at 30 kV.

X-ray Photoelectron Spectroscopy (XPS) measurements were carried out on thin 3 nm $\text{HfO}_2/\text{S}/\text{Ge}$ and $\text{Al}_2\text{O}_3/\text{S}/\text{Ge}$ stacks to ascertain the effect of S and particularly ALD oxidant on the interfacial layer (IL). The XPS core-levels (CLs) were acquired using an ultra high vacuum (UHV) system consisting of Al $K\alpha$ X-ray (1486.6 eV) source and a PSP Vacuum systems 5-channel HSA electron energy analyser. The reference samples for this study comprise of clean Ge, native GeO_2/Ge , S-treated Ge, 3 nm HfO_2/Ge and 3 nm $\text{Al}_2\text{O}_3/\text{Ge}$. The clean Ge sample was obtained by sputtering and in-situ annealing of a Ge(100) surface in UHV, and was considered clean when no oxygen or carbon was detected by XPS. The electron binding energies (BEs) were calibrated using the Ag 3d peaks from a clean silver foil or by setting the C 1s peak in the spectra (due to stray carbon impurities in the as-received samples from the ALD reactor) at 284.6 eV for all samples [9]. The CL spectra were fitted using Gaussian-Lorentzian lineshapes with a Shirley-type background [10].

For electrical measurements, gold contacts were deposited on 7 nm HfO_2 films to form MOS gate electrodes, while Al was deposited on the back of the Ge wafers to provide an Ohmic contact. The capacitance voltage (CV) measurements in the

frequency range of 1-400 kHz were performed to estimate the effect of different passivation methods on the interfacial layer.

3. Results and Discussion

3.1 Interfacial Features of Hafnia on Sulphur Passivated Germanium

Figure 1 shows a comparison of the Ge 3d lineshape measured from several samples. The XPS Ge 3d CL spectrum for a sample of clean Ge is shown in Fig. 1(a). The experimental curve is fitted with two sub-peaks corresponding to Ge $3d_{5/2}$ at 29.42 eV and Ge $3d_{3/2}$ at 30.37 eV, corresponding to the spin-orbit doublet. Compared to the spectrum of clean Ge sample, the S-treated Ge sample in Fig. 1(b) shows an additional feature, which is also fitted with a doublet. This feature is at ~ 0.9 eV chemical shift from Ge 3d substrate peak and can be attributed to GeS species in agreement with the literature [4].

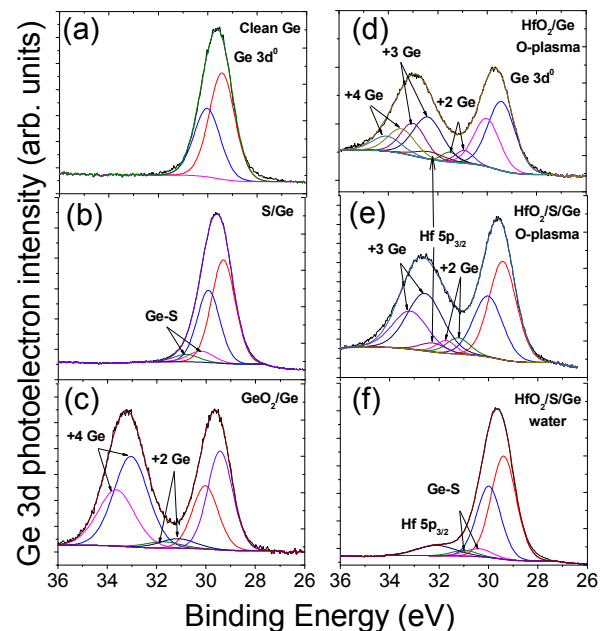


Figure 1: Ge 3d XPS core level lineshape for: (a) clean Ge, (b) S-passivated Ge, (c) native GeO_2/Ge , (d) HfO_2/Ge , (e) $\text{HfO}_2/\text{S}/\text{Ge}$ using oxygen plasma as oxidant, and (f) $\text{HfO}_2/\text{S}/\text{Ge}$ using water as oxidant during ALD deposition. The thickness of all oxide layers is ~ 3 nm.

Figure 1(c) shows the spectrum of native

GeO₂/Ge. The peak fitted at 33.03 eV is attributed to the +4 Ge oxidation state (i.e. GeO₂), while a small peak centred around 1.7 eV above the Ge 3d⁰ (indicated on the figure with arrows) is related to +2 Ge oxidation state (i.e. GeO) [11]. Comparing with the sulphur treated sample, it is apparent that the addition of sulphur is very effective in passivating the sample, as evidenced by the absence of the GeO₂ peak in Fig. 1(b).

Fig. 1(d) and 1(e) show the Ge 3d lineshape from hafnia grown using oxygen plasma without and with S-pretreatment respectively. The effect of O-plasma is increased presence of GeO_x, in particular +2 Ge, as indicated by the increased intensity in the region between the two main peaks, at ~ 31 eV. This is evident when comparing with Fig. 1(c) where the sample had predominantly the GeO₂ layer on Ge. Binding energy differences lower than 3.4 eV in Figs. 1(d)-(e) indicate either HfGeO or the occurrence of Ge in oxidation states lower than +4 [12]. The former has been excluded since the chemical shift observed (~3 eV) is larger than reported for HfGeO (2.45 eV) [13]. Furthermore, there is no appreciable shift of Hf 4f peaks for both samples in Figs. 1(d)-(e) [14]. The chemical shift value is close to reported 2.9 eV for +3 Ge oxidation state [4]. It can be seen that the overall lineshape due to the GeO₂ peak (see Figs. 1(d)-(e) in comparison to Fig. 1(c)) is broadened, together with the presence of Hf 5p_{3/2} peak from HfO₂ at ~ 32 eV as indicated by the arrows. Note also slight narrowing of IL sub-peak and dominance of +3 Ge species for O-plasma HfO₂/Si/Ge in comparison to HfO₂/Ge. Figure 1(f) shows the Ge 3d XPS spectrum for HfO₂ taken from sample made on S-passivated Ge using water as the oxidant. It is apparent that the GeO₂ and GeO_x peaks are significantly suppressed for the latter sample. Thus, it is possible to conclude that hafnia deposited on S-passivated samples using water does not induce a reaction with germanium to produce significant amounts of GeO_x. On the other hand, despite S-passivation, oxygen plasma seems more aggressive during hafnia growth and induces significant GeO_x (+2 Ge and +3 Ge) formation.

The HfO₂ layers on Ge deposited using O-plasma were found to be amorphous. Figure 2 shows a typical TEM image of a 20 nm HfO₂ on Ge.

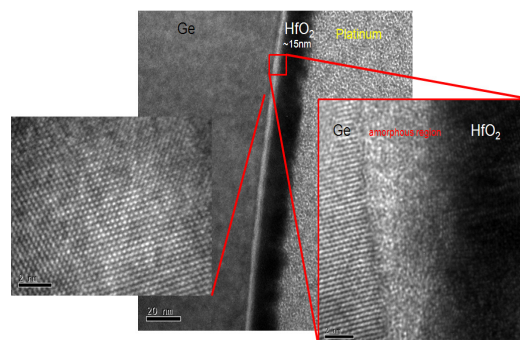


Figure 2: The cross-section TEM image of 20 nm HfO₂/Ge deposited by ALD using O-plasma oxidant.

The image shows the crystalline nature of the Ge substrate and the amorphous HfO₂ and IL.

3.2. Interfacial Features of Al₂O₃ on Sulphur Passivated Germanium

Figure 3 shows the Ge 3d XPS spectra for 3 nm Al₂O₃/Ge stacks deposited with and without sulphur passivation.

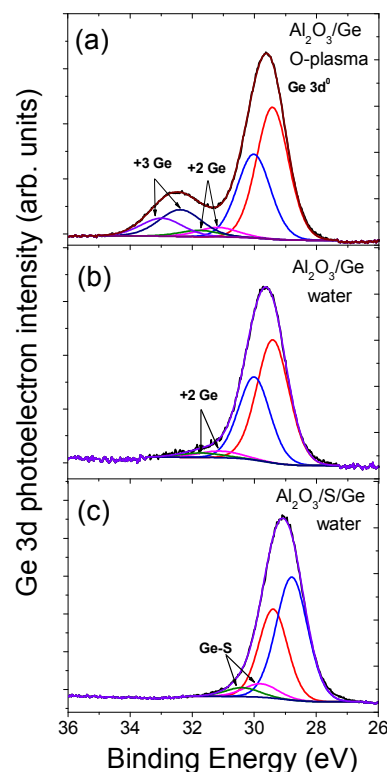


Figure 3: Ge 3d XPS core level for (a) Al₂O₃/Ge using O-plasma, (b) Al₂O₃/Ge using water, and (c) Al₂O₃/S/Ge using water as oxidants during ALD.

The experimental curve fitting procedure was the same as for that shown in Fig. 1. Figures 3(a) and 3(b) show the Ge 3d core levels from Al_2O_3 grown on Ge substrate using oxygen plasma and using water as oxidants respectively, both without S-pretreatment. Note narrower IL sub-peak for $\text{Al}_2\text{O}_3/\text{Ge}$ stack in Fig. 1(a) than for the same thickness HfO_2/Ge stack in Fig. 1(d). This is in agreement with experimentally [1] and theoretically [15] observed lower reactivity of alumina on Ge than hafnia on Ge. It can be seen in Fig. 3(a) that the effect of the oxygen plasma is a significant presence of both +3 Ge (at ~ 3 eV chemical shift) and +2 Ge (at 1.7 eV), compared to the sample grown using water as the oxidant in Fig. 3(b). It is evident from Fig. 3(c) that S-pretreatment in combination with depositing alumina with water prevents the formation of GeO_x . There is a clear Ge-S doublet peak at ~ 0.9 eV chemical shift in agreement with the observation in Fig. 1(f), as a fingerprint of Ge-S bond at the interface. The results from Fig. 3 suggest that samples prepared by ALD using H_2O have much reduced GeO_x species, and this improves further if the Ge is pretreated with S.

3.3 The Effect of S and S/sub-nm Al_2O_3 passivation on CV characteristics of HfO_2/Ge stacks

The capacitance voltage characteristics for 7 nm HfO_2/Ge stacks deposited by ALD using O-plasma are shown in Fig. 4. Two types of passivation treatments on Ge, namely S (open square symbol in Fig. 4) and S/0.3 nm Al_2O_3 (triangle symbol curve in Fig. 4) were compared to the CV results from HfO_2/Ge sample without any passivation (open circle symbol curve in Fig. 4). The CV results were plotted for two frequencies 50 and 100 kHz. There is evidence of the frequency dependence of the distortion in the CV, around 0.5 V for the HfO_2/Ge sample and ~ -0.5 V for $\text{HfO}_2/0.3$ nm $\text{Al}_2\text{O}_3/\text{S}/\text{Ge}$ sample indicated by the arrows in Fig. 4. There is a slight shift of these humps to lower voltages with decreasing measuring frequency to 50 kHz. This behaviour is consistent with the response of interfacial defects located in the energy gap at the insulator/semiconductor interface [16,17]. Note that such behaviour is not evident for S-passivated Ge stack (see open square curves in Fig. 4). The electrical quality of the interface has been found to strongly depend on the Ge oxidation states [18,19].

Houssa et al. [20] have found from the first principles calculations that the formation of Ge–O bonds or Hf–O–Ge bonds at or near the HfO_2/Ge interface does not result in the presence of surface states in the Ge energy band gap. However, the formation of a metallic Ge–Hf bond at the interface, likely present if Hf is located in the sub-oxide interfacial layer (GeO_x with $x < 2$), has been shown to result in the formation of a defect level in the upper part of the Ge energy band gap, hampering the electrical properties of MOS devices. Referring to our XPS results in Figs. 1(d) and 1(e), there is no evidence of +1 Ge oxidation species, and even for $\text{HfO}_2/\text{S}/\text{Ge}$ stacks the presence of both +2 Ge and +3 Ge species at the interface has no detrimental effect on the CV characteristic shown in Fig. 4, where the curve is near ideal without any distortions around flat band region.

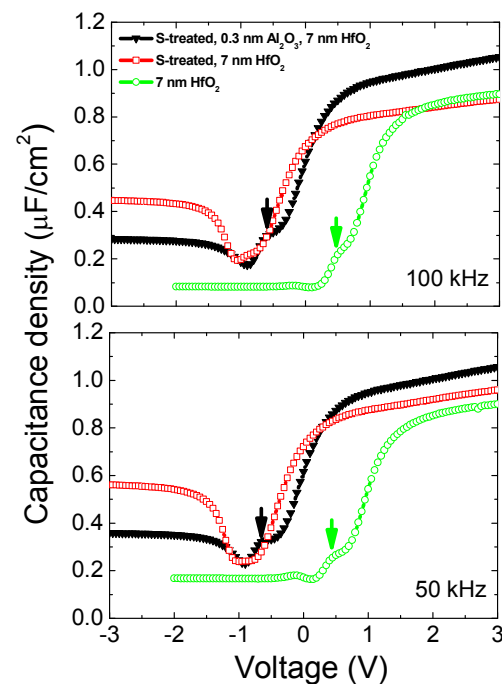


Figure 4: The CV plots at 50 and 100 kHz of 7 nm HfO_2/Ge gate stacks deposited by ALD using O-plasma as oxidant on two differently passivated Ge surfaces: S/Ge, and 0.3 nm $\text{Al}_2\text{O}_3/\text{S}/\text{Ge}$. The reference sample is HfO_2/Ge without any passivation. The arrows point to the CV distortions around flat band regions.

Hence, it seems plausible that the observation of the CV distortion in HfO_2/Ge simple (see Figs. 4 and 1(d)) does not relate to Hf-Ge bonds, but could rather originate from extrinsic defects. For the sample with

HfO₂/0.3 nm Al₂O₃/S/Ge the CV distortion is less pronounced. Note also that the latter gate stack is the most scalable, as it shows the highest value of accumulation capacitance.

From the CV characteristics for HfO₂/S/Ge simple in Fig. 4, the capacitance equivalent thickness (CET) of 2.7 nm can be calculated from the maximum (accumulation) capacitance. Assuming permittivity of 21.3 for HfO₂, estimated previously from the variation of CET as a function of HfO₂ thickness [21], the equivalent oxide thickness (EOT) of IL for HfO₂/S/Ge stacks is estimated to be 1 nm. The electrical results strongly support the case for sulphur passivation of the interface.

4. Conclusion

In this paper, HfO₂/Ge and Al₂O₃/Ge gate stacks have been deposited by atomic layer deposition using O-plasma and H₂O as oxidants. Detailed X-ray photoelectron spectroscopy results show that sulphur passivation of germanium is very effective in preventing the formation of the GeO_x at the interface, in particular if the ALD oxidant is water when depositing either 3 nm HfO₂ or Al₂O₃ films. Furthermore, the interfacial +3 Ge and +2 Ge species evident for HfO₂/S/Ge stack deposited using O-plasma, have been found to have no deleterious effect on the electrical quality of the interface. The results suggest the efficient passivation of Ge by sulphur, when a well controlled oxidation process is performed.

Acknowledgements

The work was funded by the EPSRC, UK, project number EP/1012907/1. One of the authors (MA) acknowledges support from Physics Department, Taif University, Saudi Arabia.

References

- [1] S. Takagi, R. Zhang, M. Takenaka, *Microelectron. Eng.* 109 (2013) 389.
- [2] Y. Oshima, M. Shandalov, Y. Sun, P. Pianetta, P.C. McIntyre, *Appl. Phys. Lett.* 94 (2009) 183102.
- [3] J.J.-H. Chen, N.A. Bojarezuk Jr., H. Shang, M. Copel, J.B. Hannon, J. Karasinski, E. Preisler, S.K. Banerjee, S. Guha, *IEEE Trans. Electron Devices* 51 (2004) 1441.
- [4] R. Chellappan, D. Gajula, D. McNeill, G. Hughes, *Appl. Surf. Sci.* 292 (2014) 345.
- [5] R. Chellappan, D. Gajula, D. McNeill, G. Hughes, *J. Appl. Phys.* 114 (2013) 084312.
- [6] S. Sioncke, J. Ceuppens, D. Lin, L. Nyns, A. Delabie, H. Struyf, S. De Gendt, M. Muller, B. Beckhoff, and M. Caymax, *Microelectron. Eng.* 88 (2011) 1553.
- [7] S. Sioncke, H.C. Lin, L. Nyns, G. Brammertz, A. Delabie, T. Conard, A. Franquet, J. Rip, H. Struyf, S. De Gendt, M. Muller, B.

- Beckhoff, and M. Caymax, *J. Appl. Phys.* 110 (2011) 084907.
- [8] V.V. Afanas'ev, A. Stesmans, A. Delabie, F. Bellenger, M. Houssa, and M. Meuris, *Appl. Phys. Lett.* 92 (2008) 022109.
- [9] J.C. Vickerman, *Surface analysis*, (Wiley) 1998.
- [10] D.A. Shirley, *Phys. Rev. B* 5 (1972) 4709 (1972).
- [11] T. Sasada, Y. Nakakita, M. Takenaka, S. Takagi, *J. Appl. Phys.* 106 (2009) 073716.
- [12] A. Delabie, A. Alian, F. Bellenger, M. Caymax, T. Conard, A. Franquet, S. Sioncke, S. Van Elshocht, M.M. Heyns, M. Meuris, *J. Electrochem. Soc.* 156(10) (2009) G163.
- [13] O. Renault, L. Fourdrinier, E. Martinez, L. Clavelier, C. Leroyer, N. Barrett, C. Crotti, *Appl. Phys. Lett.* 90 (2007) 052112.
- [14] S. Van Elshocht, M. Caymax, T. Conard, S. De Gendt, I. Hoflijck, M. Houssa, B. De Jaeger, J. Van Steenberghe, M. Heyns, M. Meuris, *Appl. Phys. Lett.* 88 (2006) 141904.
- [15] H. Li, L. Lin, J. Robertson, *Appl. Phys. Lett.* 101 (2012) 052903.
- [16] B.J. O'Sullivan, P.K. Hurley, C. Leveugle, and J.H. Das, *J. Appl. Phys.* 89 (2001) 3811.
- [17] P.K. Hurley, K. Cherkaoui, E. O'Connor, M.C. Lemme, H.D.B. Gottlob, M. Schmidt, S. Hall, Y. Lu, O. Bui, B. Raelis, J. Piscator, O. Engstrom, and S.B. Newcomb, *J. Electrochem. Soc.* 155(2) (2008) G13.
- [18] D. Kuzum, T. Krishnamohan, A.J. Pethe, A.K. Okyay, Y. Oshima, Y. Sun, J.P. Mc Vittie, P.A. Pianetta, P.C. McIntyre, and K.C. Saraswat, *IEEE Electron. Dev. Lett.* 29 (2008) 328.
- [19] T.J. Grassman, S.R. Bishop, and A.C. Kummel, *Surf. Sci.* 602 (2008) 2373.
- [20] M. Houssa, G. Pourtois, M. Caymax, M. Meuris, M.M. Heyns, *Surf. Sci.* 602 (2008) L25.
- [21] I.Z. Mitrovic, A.D. Weerakkody, M. Althobaiti, V.R. Dhanak, N. Sedghi, S. Hall, S. Mather, P.R. Chalker, A. Dimoulas, C. Henkel, E. Dentoni Litta, P.-E. Hellström, M. Östling, *ECS Trans.* 61(2) (2014) 73; S. Mather, N. Sedghi, M. Althobaiti, I.Z. Mitrovic, C. Dhanak, P.R. Chalker, S. Hall, *Microelectron. Eng.* 109 (2013) 126.